

Ion imprinted polymer monoliths as adsorbent materials for the removal of Hg(II) from real-time aqueous samples

Siti Khadijah Ab. Rahman¹, Nor Azah Yusof^{1,2,*}, Faruq Mohammad^{3,*}, Abdul Halim Abdullah¹ and Azni Idris⁴

¹Chemistry Department, Faculty of Science,

²Institute of Advanced Technology, and

⁴Chemical Engineering and Environmental Department, Faculty of Engineering, Universiti Putra Malaysia, Serdang, Selangor, Malaysia 43400

³Surfactant Research Chair, Department of Chemistry, College of Science, King Saud University, P.O. Box 2455, Riyadh 11451, Saudi Arabia

Ion imprinted polymer monoliths (IIMs) for the adsorption of Hg(II) ions in tablet form were prepared by forming a mercury ion (template ion) complex with 2-(methacryloyloxy)ethyl trimethylammonium cysteine (ligand) and thermally copolymerized with a monomer (methacrylic acid), cross-linker (ethylene glycol dimethacrylate), initiator (benzoyl peroxide) and porogen (acetonitrile) in the polyethylene tube (drinking straw) as a mould. The formed composite was thoroughly characterized by means of FTIR, TGA, FESEM and BET, and further tested by applying the changes in solution pH, concentration, contact time, recycle test and selectivity. The analysis revealed that the activity of the materials was maximum at pH 4.7 and adsorption capacity of Hg(II) by IIMs followed the Langmuir isotherm model. The adsorption equilibrium was achieved after 120 min and followed the second-order reversible kinetics. In addition, we found that the IIMs were reusable up to 15 cycles and exhibited good selectivity towards the Hg(II) ions even in the presence of other interference ions such as Pb(II), Cd(II), As(II) and Cr(III). On further testing for the recovery of Hg(II) ions in real-time aqueous samples (contaminated petrochemical and mining industries), the IIM tablets showed higher selectivity and excellent reusability. In summary, we indicate that the IIMs are easy to prepare, possess high levels of permeability, porosity and selectivity, and offer excellent reusability, thereby making them one of the promising candidates for the successful removal of mercury ions from industrial samples.

Keywords: Adsorbent material, ion imprinted polymer monoliths, mercury ions selectivity, waste-water treatment.

MERCURY (Hg) is one among many different toxic heavy metal contaminants commonly found in the environment,

where its toxicity effects have been studied well for centuries¹. The principal anthropogenic sources of mercury contamination in the environment are the petrochemical industries², urban releases, agricultural wastes, mining and coal combustion effusions, industrial expulsions³, metal refining, manufacturing and chloralkali production units⁴, to mention a few. The released mercuric compounds undergo complex transformations in the environment that can be physical, chemical or biological. The effects of mercury or its ions in the feeds of processing systems can be system degeneration, toxic waste production and catalyst poisoning. All these factors reduce the quality of the final products, in addition to the health risk and safety of workers⁵. When the mercury from industries gets deposited in waterways, anaerobic bacteria convert it into methyl-mercury⁶, which is more toxic and participates further in a protein-binding reaction in the organisms. In another approach, mercury toxicity influences human health by entering the food chain through its accumulation in fish^{3,6}. The symptoms of Hg poisoning can be numerous and come into action either immediately or after a prolonged period of time. The high exposure of mercury can cause kidney dysfunction, respiratory failure and even death⁷.

In recent years, solid-phase extraction (SPE) is a commonly applied method for the separation of heavy metal ions due to its attractive features such as safety, flexibility, economy, nature-friendly, free of emulsion, fast, accuracy, ease of sampling and automation⁸. Also, the SPE method by the use of ion imprinted polymers (IIPs) is the most popular approach for the preconcentration and recovery of trace metals⁹. The IIPs have been identified as highly suitable materials for the selective adsorption of toxic metal ions in the SPE approach⁸. Using IIPs as adsorbents is the most suitable method for removing Hg(II) ions from the aqueous waste-water samples due to the high amounts of loading, enhanced selectivity, specificity, low cost and easy method of preparation¹⁰.

The most widely used method for the preparation of IIPs in particulate form is the traditional polymerization

*For correspondence. (e-mail: azahy@upm.edu.my; fmohammad@ksu.edu.sa)

method, where the bulk IIPs need to be crushed first followed by grinding and sieving through a mesh. The particles formed are mostly irregularly shaped with varying sizes and this significantly reduces the adsorption efficiency. In order to overcome this, spherical IIPs are formed by different methods, including the swelling method^{11,12}, suspension and precipitation polymerization¹³ and surface imprinting on the spherical polymer or silica¹⁴. Similarly, the ion imprinting polymer monoliths (IIMs) are prepared using the moulding technique, as the strategy enables to directly synthesize the IIMs formed with enhanced resolution, low back pressure and enriched flow rate. Furthermore, the amount of template ions used for the preparation of IIMs in the moulding technique is far less compared to other synthesis techniques. In addition, the IIMs formed display enhanced porosity, enriched permeability and higher surface areas¹⁵.

In the present study, 2-(methacryloyloxy)ethyltrimethylammonium cysteine (MAETC) has been chosen as the metal complexing monomer. The preparation of Hg(II) imprinted polymethacrylic acid MAETC monolithic IIMs in tablet form was done using 0.5% thiourea per 0.05 M HCl solution. The IIMs formed were characterized using Fourier-transform infrared spectroscopy (FTIR), field emission scanning electron microscopy (FESEM), thermo-gravimetric analysis (TGA), Barrett–Joyner–Halenda (BJH) and Brunauer–Emmett–Teller (BET) analysis. For the testing of IIMs, adsorption of Hg(II) ions from the aqueous solutions was investigated by applying the changes in terms of pH, concentration, contact time, selectivity for Hg(II) and reusability. Further, the synthesized IIMs were tested for separation of Hg(II) ions from different industrial water samples that included the contaminated mining and petrochemical industries.

Materials and methods

Reagents

An aqueous solution stock in the range 10–400 µg/l was prepared by diluting 1000 mg/l of standard mercury nitrate (Hg(NO₃)₂) (Sigma Aldrich, USA) in deionized water (obtained with a thermo scientific water system, Barnstead Nanopure, Waltham, Massachusetts, USA) using a volumetric flask. Sodium nitrate (NaNO₃), potassium carbonate (K₂CO₃), ethyl acetate, thiourea, sodium hydroxide (NaOH), L-cysteine, ethylene glycol dimethacrylate (EGDMA), 2-hydroxyethyl methacrylate (HEMA) and methacryloyl(oxyethyl)trimethyl ammonium chloride (MOTAC) were purchased from Sigma Aldrich. Methacrylic acid (MAA), cadmium standard for AAS and lead standard for AAS were purchased from Fluka, Shanghai, China. Acetonitrile (ACN), benzoyl peroxide (BPO) and nitric acid (HNO₃) were the products of R&M Chemicals, Selangor, Malaysia. Methanol, hy-

drochloric acid (HCl) and ethanol were obtained from J.T. Baker, Selangor, Malaysia. Chromium (III) nitrate (Cr(NO₃)₃) and arsenic trichloride standard for AAS were obtained from Spectrosol, USA. Polyethylene tubes (drinking straw) were purchased from a local departmental store (Seri Kembangan, Selangor, Malaysia) and river water (contaminated mining of bauxite industry) was collected from Balok, Kuantan, Pahang, Malaysia. Waste water and condensate (contaminated petrochemical industry) were collected from Kerteh, Terengganu, Malaysia.

Synthesis of MAETC ligand

The synthesis of MAETC as a ligand is important to produce the required IIMs. The experimental procedure was conducted as follows: 5 g of cysteine and 0.2 g of sodium nitrate were dissolved in 30 ml of K₂CO₃ aqueous solution (5% v/v), followed by cooling to 0°C in a refrigerator. To this solution, about 4 ml of MOTAC was added slowly, with stirring under nitrogen atmosphere for 3 h at room temperature using a magnetic stirrer. The pH was maintained at 7.0, followed by extraction using ethyl acetate. Further evaporation of the aqueous phase on a rotary evaporator resulted in the formation of crystals which were crystallized in ethanol and ethyl acetate. The MAETC product formed was dried in an oven and the dried product was transferred to the next level for the preparation of IIMs.

Preparation of IIMs

The IIMs were prepared using the thermal polymerization method by dissolving 2 mmol of MAETC and 0.5 mmol of Hg(NO₃)₂ as a template in methanol (total volume 50 ml). The solution was stirred for 2 h at room temperature. Then 5 ml of MAETC-Hg solution was pipetted into a 5 ml beaker and a series of solutions were added, such as 6 mmol MAA as functional monomer, 3 mmol HEMA as co-monomer, 30 mmol EGDMA as cross-linker, 20 ml ACN as porogen and 0.1 g BPO as an initiator. At this state, the mixture was stirred for 30 min with nitrogen gas purging and then sealed. Next, the mixture was transferred into a mould (drinking straws) which was then transferred to a water bath maintained at 70°C to undergo the polymerization process. This process was repeated for 4 h and the polymers formed were cut into small pieces.



Figure 1. Formation of ion imprinted polymer monoliths in tablet form using straws as a mould.

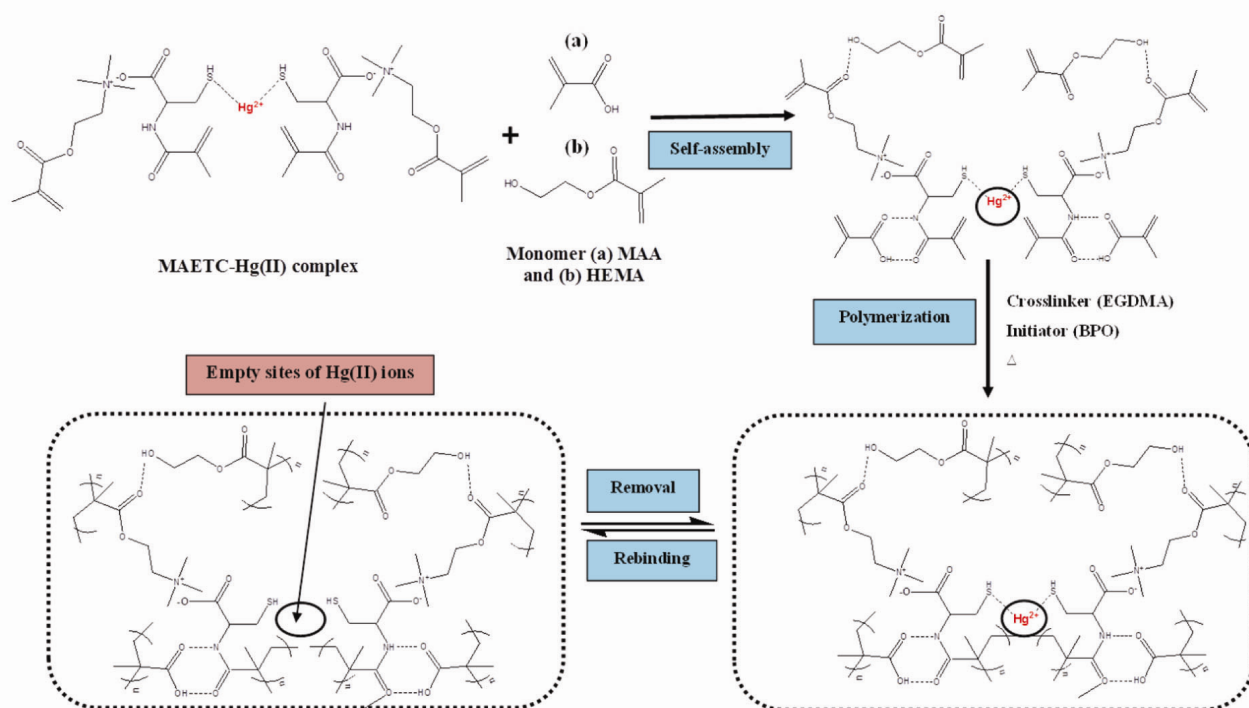


Figure 2. Proposed reaction mechanism for the preparation of IIMs.

Figure 1 shows the formation of IIMs in tablet form using drinking straws as a mould. The extraction of IIMs with methanol/water mixture (60/40 v/v) was repeated several times for removing the unreacted monomers and any other ingredients. Then, the IIMs were washed with 0.5% thiourea in 0.05 M HCl solution for the extraction of template ions (Hg(II)). This process was continued multiple times until the template ions were absent in the filtrate when tested using the inductively coupled plasma-mass spectrometry (ICP-MS) technique. The template ions of Hg(II) (free particles) were removed by washing with a solution of 0.1 M HNO₃ for 3 h. Figure 2 shows the mechanism for preparation of IIMs.

Characterization of synthesized IIMs

The FTIR spectroscopic analysis was carried out using Perkin Elmer model 100 series (CT, USA) in the infrared range 4000–200 cm⁻¹. For the analysis of samples, the IIMs were applied to universal attenuated total reflectance (UATR) technique. Thermal studies by means of TGA analyses were performed on a Metler Toledo TGA/SDTA 851e model (Metler Toledo, Greifensee, Switzerland). The surface morphology studies by means of FESEM analyses were performed using a JEOL-JSM-7600F model (Tokyo, Japan) operated at an accelerating voltage of 5 kV. The BET surface area analyses for the IIM samples were done by performing nitrogen adsorption at liquid nitrogen temperature (77 K) using Auto-

sorb-1 instrument controlled by Quantachrome AS1Win software. Typically, 0.008–0.010 g of IIM sample was used each time for the surface area analysis. Further, the ICP-MS measurements were performed by ELAN DRC-e spectrometer (Perkin Elmer SCIEX, Concord, Ontario, Canada) controlled by ELAN instrumental software.

Adsorption studies

The batch experiment technique was adopted for adsorption of Hg(II) ions from aqueous solutions. The IIM adsorption effects against the changes in pH, isotherm, contact time, effect of foreign ions, recycle test and further application towards real-time samples were studied. The adsorption capacity was calculated using the equation

$$q = \frac{(C_0 - C_e) \times V}{M}, \quad (1)$$

where q (μg/g) is the total amount of Hg(II) ions adsorbed, C_0 and C_e are the initial and equilibrium concentrations of the Hg(II) ions (μg/l), V (l) the total solution volume and M is the total weight (g) of the IIMs. For the study, the IIMs were first placed in a column which was conditioned with 2 ml each of deionized water and methanol; this was followed by passing of the test sample through the column and then collecting it at the

bottom. The initial (C_0) and final (C_e) concentration of Hg(II), Cr(III), Pb(II), As(II) and Cd(II) were determined using the ICP-MS instrument.

The effect of pH on the adsorption of Hg(II) ions by the IIMs (0.1 g) was studied using 10 $\mu\text{g/l}$ of Hg(II) solution (0.1 l) with the adjustment of pH values (2.0, 3.0, 4.0, 5.0, 6.0, 8.0 and 10.0). The same parameters were used for testing the adsorption at pH 4.7 also. The sorption isotherm was measured using 0.1 g of IIMs in 0.1 l of Hg(II) solution with various concentrations (5, 10, 20, 50, 100, 200 and 400 $\mu\text{g/l}$). The effect of time on the adsorption of Hg(II) was studied using 0.21 l of Hg(II) solution treated with 0.21 g of IIMs. The treated samples were collected at various time intervals (2, 5, 10, 20, 40, 60 and 120 min). In addition, the selectivity of IIMs towards Hg(II) ions over other metal ions was also studied. A solution (0.1 l) containing 10 $\mu\text{g/l}$ of Hg(II), Cr(III), Pb(II), As(II) and Cd(II) was mixed together and treated with 0.1 g of IIMs. For the recycle test, 0.1 l of Hg(II) solution (10 $\mu\text{g/l}$ and pH 4.7) was treated with 0.1 g of IIMs. Following the collection of treated samples, the IIMs were washed several times with 0.5% thiourea in 0.05 M HCl solution. Then, they were dried and weighed before proceeding to the next recycling. The IIMs were also applied for real-time samples such as waste water, condensate (collected from petrochemical industry, Kerteh, Terengganu, Malaysia) and river-water samples (collected from Balok, Pahang, Malaysia) in this study. The waste water, condensate and river-water samples were centrifuged for 10 min (3000 rpm) and filtered to separate the supernatant and oil residue, and the filtered samples (0.1 l) were treated with IIMs (0.1 g) for adsorption studies.

Results and discussion

Physical characterization of IIMs

FTIR of IIMs: Figure 3 shows the FTIR spectra of monomer-MAA, MAETC and IIMs. From the figure, the medium intensity of N–H amines in MAETC can be observed for MAETC and IIMs spectra at 3371 and 3449 cm^{-1} respectively, but this peak seems to be missing for the monomer-MAA. The broad O–H stretch peak for monomer-MAA and MAETC can be observed at 2923 and 2774 cm^{-1} respectively. The O–H stretch peak can also be observed for the IIMs at 2960 cm^{-1} , but the intensity of this peak is smaller compared to monomer-MAA and MAETC. This indicates the formation and interaction of hydrogen bonding between the monomer-MAA and MAETC compounds that has occurred during the polymerization process. The intensity of the broad intermolecular hydrogen-bonded band is reduced considerably, leaving the major band, the free O–H stretching absorption. The spectrum of MAETC shows the characteristic absorbance peak around 2550 cm^{-1} which can be ascribed

to S–H (thiol group) vibrations. However, the S–H peak for the IIMs disappears in the spectra due to the sulfhydryl groups, where they can donate a lone pair of electrons to the empty Hg(II) orbitals, thereby confirming for the formation of MAETC–Hg complex. In addition, all the spectra showed the formation of C=O and C–O of carboxylic groups in the monomer-MAA, MAETC and IIMs compounds; the C=O stretching band appeared at 1690, 1731 and 1720 cm^{-1} , while the C–O band at 1199, 1290 and 1150 cm^{-1} for monomer-MAA, MAETC and the IIMs respectively. A stronger and sharper peak could be observed for the IIMs compared to the monomer-MAA and MAETC compounds, this is due to the existence of C=O and C–O bonds in the EGDMA compound as cross-linker. In the spectrum of monomer-MAA, the C=C bond peak found at 1630 cm^{-1} is absent in the spectrum of IIMs, thereby confirming the complete polymerization of monomer-MAA.

Thermal stability of IIMs: Figure 4 shows a comparison of TGA data for MAETC, monomer-MAA and IIMs. For

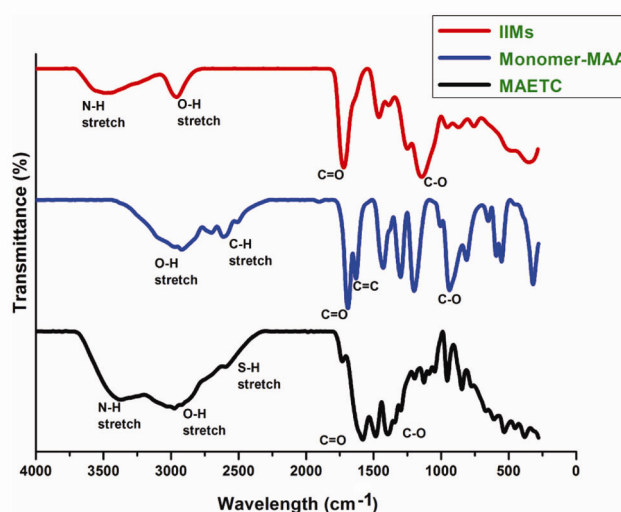


Figure 3. FTIR spectra for monomer-MAA, MAETC and IIMs.

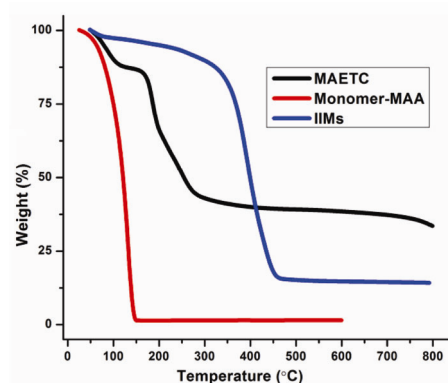


Figure 4. TGA curves for MAETC, monomer-MAA and IIMs.

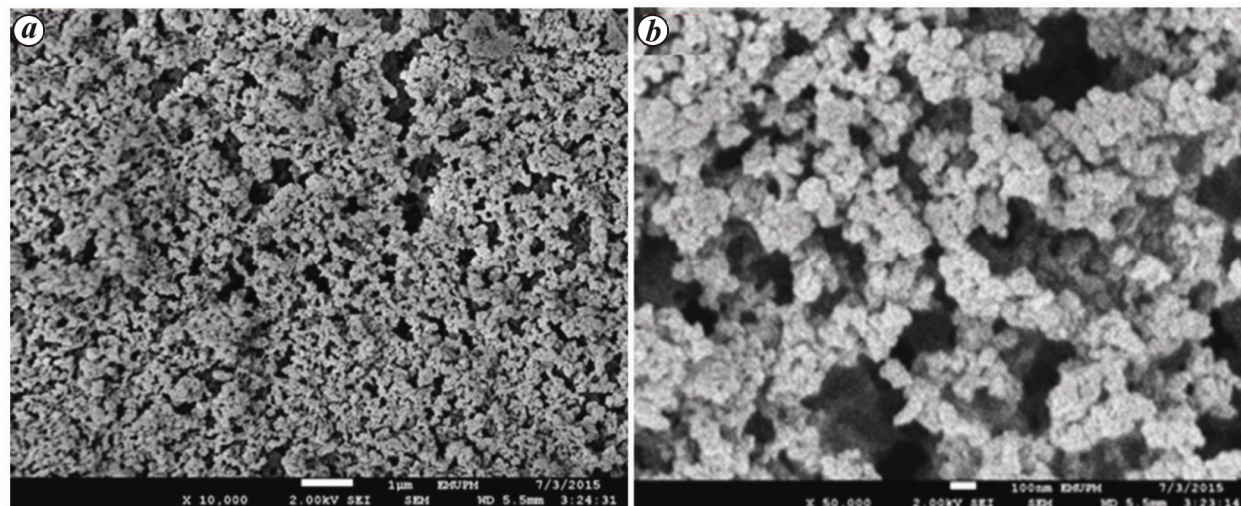


Figure 5. Surface morphology of the IIMs under (a) 10 K and (b) 50 K magnification.

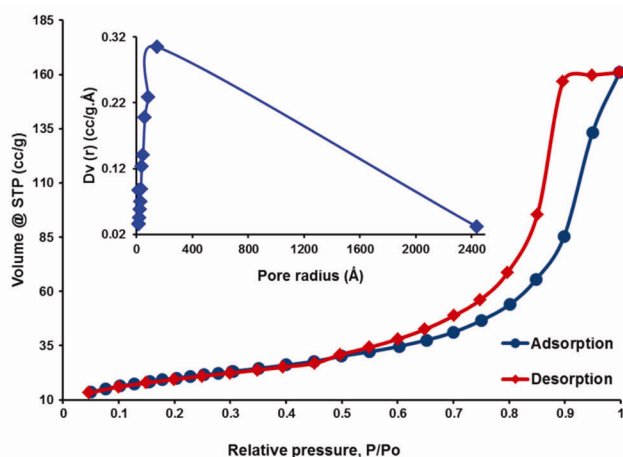


Figure 6. BET and BJH graphs for the IIMs.

the analysis, appropriate amounts of adsorbent were heated over the range 20–820°C and the weight changes were monitored. The initial decomposition temperature (T_i) of monomer-MAA and MAETC were 35°C and 133°C, while the final decomposition temperature (T_f) was 148°C and 448°C respectively. However, T_i and T_f for the IIMs was 194°C and 491°C respectively. The thermogram for the IIMs also shows that the adsorbent can withstand any weight loss up to 150°C. This indicates that the thermal stability of monomer-MAA and MAETC is lower than the IIM polymer due to their low molecular weights compared to the polymer network. From the analysis of these results, it can be confirmed that the IIMs can successfully be employed as adsorbents even at high temperature conditions.

Morphology of IIMs: Figure 5 a and b shows the surface morphology of the prepared IIMs under 10,000 and

50,000 magnification respectively. The figure clearly indicates that there are many mesopores and flow-through pores in the skeleton. The globular, aggregated, cross-linked and porous structure in the IIMs indicate that they have the ability to provide flow paths through the monolithic polymers and would be beneficial for ionic adsorption/desorption purposes.

Surface area and porosity of IIMs: The surface area and porosity analyses were performed by nitrogen adsorption–desorption method. Figure 6 shows the typical BET nitrogen sorption isotherms and overlap with the typical BJH adsorption pore size distribution curves of the IIMs. The analysis shows that the adsorbents follow the typical ‘type IV’ adsorption–desorption isotherm, this is in agreement with the capillary condensation phenomenon that usually occurs in the mesoporous materials. The BJH curves also show mesoporous material with a pore size diameter of around 3.82 nm. These pores allow Hg(II) ions to flow through the IIMs with a very low flow resistance. Moreover, the IIMs have a large specific surface area (73.16 m²/g) and average pore volume (0.24 cm³/g).

Adsorption studies

Effect of pH: Figure 7 shows the effect of pH towards the adsorption capacity of Hg(II) ions by the IIMs. The figure indicates that the adsorption capacity increases rapidly with an increase in pH in the 2.0–4.7 range, while it decreases at pH > 4.7. At pH < 5, more H⁺ ions are available in the solution which mostly prevent the Hg(II) ions from entering the adsorption sites of the IIMs. In other words, the higher H⁺ concentration in the sample solution results in the generation of positively charged IIMs, which mostly decreases the adsorption capacity of the IIMs by reducing the interactions between the IIM

sites and the Hg(II) ions¹⁶. However, decrease in the adsorption capacity of the IIMs at pH > 5 is expected and is mostly due to an increase in the number of species like OH⁻ and Hg(OH)₂ in the solution¹⁷. In addition, the negatively charged surface of the IIMs makes it difficult for the major Hg(II) species present to bind due to the electrostatic repulsions created. Also, the maximum adsorption takes place at pH 4.7 (original pH) and at this pH, the adsorption capacity of Hg(II) is high due to the presence of dominant soluble Hg(II) ions in solution. Therefore, pH 4.7 was selected as optimal for subsequent analyses.

Isotherm study: Isotherm study investigates the effect of concentration towards the adsorption capacity. We plotted the concentration of Hg(II) adsorbed onto the IIM sites versus Hg(II) free (initial concentration of Hg(II)) in solution¹⁸. Figure 8 shows the adsorption capacity of Hg(II) ions removal at a range of concentrations (5, 10, 20, 40, 60, 80 and 200 µg/l) with 0.1 g of adsorbent. The total uptake of Hg(II) ions increased with an increase in

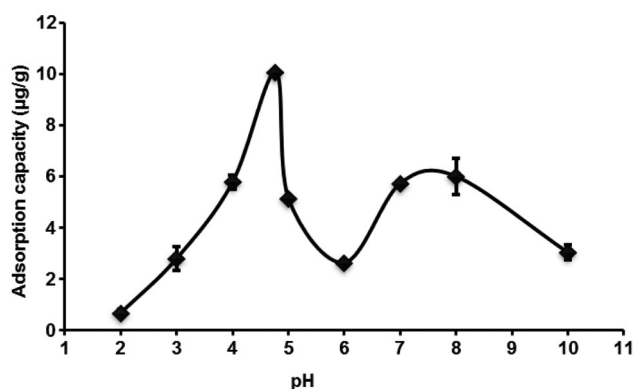


Figure 7. Comparison of the effect of pH on the adsorption of Hg(II) ions by the IIMs (experimental conditions: 0.1 g of IIMs; $C_{\text{Hg(II)}}$ 10 µg/l; volume 0.1 l; room temperature).

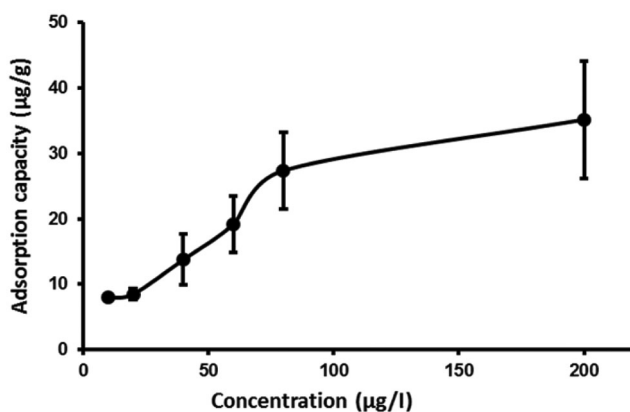


Figure 8. Effect of concentration on the adsorption of Hg(II) ions by the IIMs (experimental conditions: 0.1 g of IIMs; $C_{\text{Hg(II)}}$ 50 µg/l; volume 0.1 l; pH 4.7; room temperature).

their concentration. The saturation point or maximum adsorption capacity (35.15 µg of Hg(II)/g) was achieved at 200 µg/l of initial concentration of Hg(II) ions per 0.1 g of IIMs. Then, the adsorption data obtained were fitted to two well-known adsorption models, Langmuir and Freundlich isotherm models.

These two models are generally used to explain adsorption equilibrium over the entire studied concentration range. In the Langmuir model, adsorption is assumed to occur uniformly on the active sites of the IIMs by assuming a monolayer adsorption¹⁸. The Langmuir isotherm is represented by the equation¹⁹

$$\frac{C_e}{q_e} = \frac{1}{K_L b_L} + \frac{C_e}{K_L}, \quad (2)$$

where q_e is the concentration of Hg(II) ions adsorbed by the IIMs at equilibrium (µg/g), C_e the concentration of Hg(II) ions at equilibrium (µg/l), K_L the maximum monolayer sorption capacity of the sorbent (µg/g) and b_L is the Langmuir isotherm constant related to energy of sorption (1/µg). The linearity of the plot indicates the capability of the Langmuir isotherm.

However, based on the multilayer adsorption (heterogeneous surface), the Freundlich isotherm provides a relationship between the equilibrium liquid and solid phase capacity¹⁸. The linear equation can be expressed as¹⁹

$$\ln q_e = \ln K_F + b_F \ln C_e. \quad (3)$$

where K_F stands for the adsorption capacity (µg/g), b_F the empirical parameter related to adsorption intensity. Figure 9a and b shows the graph of Langmuir and Freundlich isotherm Hg(II) ions sorption by the IIMs. The graph is linear with a slope of $1/K_L$ and intercept of $1/K_L b_L$, where K_L gives the theoretical monolayer saturation capacity. The b_F constant can be calculated from the slope of the graph, while K_F can be calculated from the interception value at y-axis.

Table 1 provides both parameters obtained by Langmuir and Freundlich models for the adsorption of Hg(II) ions by the IIMs. Based on the table, the Langmuir model has higher correlation coefficient ($R^2 = 0.951$) compared to the Freundlich model ($R^2 = 0.876$). The K_L value calculated (37.313 µg/g) by making use of the Langmuir model is close to experimental q_{max} value (35.151 µg/g), as against the K_F value (5.243 µg/g) obtained from Freundlich model. From the analysis therefore, it can be concluded that the IIMs adsorption of Hg(II) ions are following the Langmuir isotherm model, and the adsorption phenomenon is monolayer (homogeneous surface).

Effect of time: Effect of time or kinetic study is an important parameter required for investigating the adsorption rate of Hg(II) ions at the available binding sites of

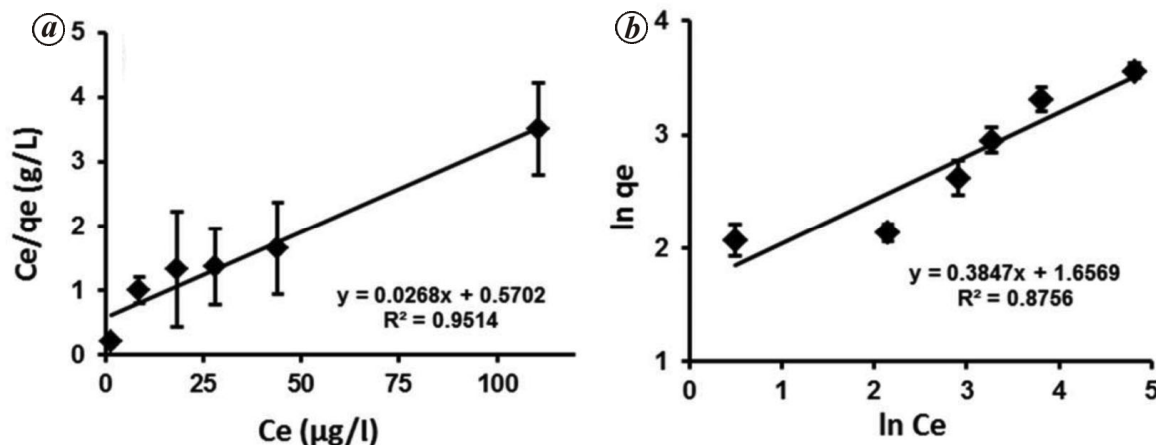


Figure 9. (a) Langmuir and (b) Freundlich isotherm models for adsorption of Hg(II) ions by the IIMs.

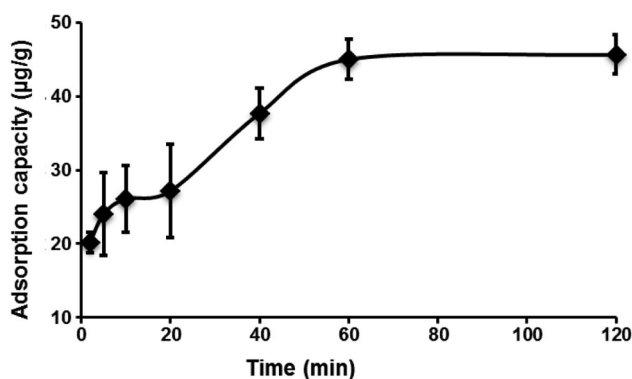


Figure 10. Effect of time on the adsorption of Hg(II) by IIMs (experimental conditions: 0.21 g of IIMs; $C_{\text{Hg(II)}}$ 50 µg/l; volume 0.21 l; pH 4.7; room temperature).

the IIMs. Figure 10 shows a comparison of Hg(II) ions adsorption by the IIMs over a range of time (2–120 min) when the other parameters are constant. The graph indicates that the adsorption capacity increases with respect to time for the first 60 min and further increase in time makes the Hg(II) adsorption constant, which approaches an equilibrium when the adsorption time is increased further. The highest adsorption of Hg(II) ions by the IIMs is 45.63 µg/g at 120 min. The adsorption data obtained were analysed using first- and second-order kinetic models.

The first-order rate model (eq. (4)) was used for analysing the sorption kinetic model as²⁰

$$\frac{dq}{dt} = k_1(q_e - q). \tag{4}$$

After the definite integration and by applying the initial condition $q = 0$ at $t = 0$ to eq. (4), we get²⁰

$$\ln(q_e - q) = \ln q_e - k_1 t. \tag{5}$$

where q_e and q denote the adsorption capacity of Hg(II) ions (µg/g) at equilibrium and at time t respectively, and k_1 is the first-order rate constant (min^{-1}). Figure 11 a shows the pseudo first-order model for the sorption of Hg(II) ions by the IIMs. k_1 can be calculated from the slope of the graph, while the q_e can be obtained from the interception value at the y-axis.

By making use of the pseudo second-order equation (eq. (6)), the sorption kinetics data for the adsorption of Hg(II) ions were also analysed²⁰

$$\frac{dq}{dt} = k_2(q_e - q)^2. \tag{6}$$

On integration of the above equation and further application of the initial parameters, we get²⁰

$$\frac{t}{q} = \frac{1}{q_e^2 k_2} + \frac{t}{q_e}, \tag{7}$$

where q_e is the adsorption capacity of Hg(II) ions at equilibrium (µg/g), k_2 the second-order rate constant (min^{-1}) and q is the adsorption capacity (µg/g). Figure 11 b shows the pseudo second-order model for the sorption of Hg(II) ions by the IIMs. The value of k_2 can be calculated from the slope of graph, while q_e can be calculated from the interception value at the y-axis.

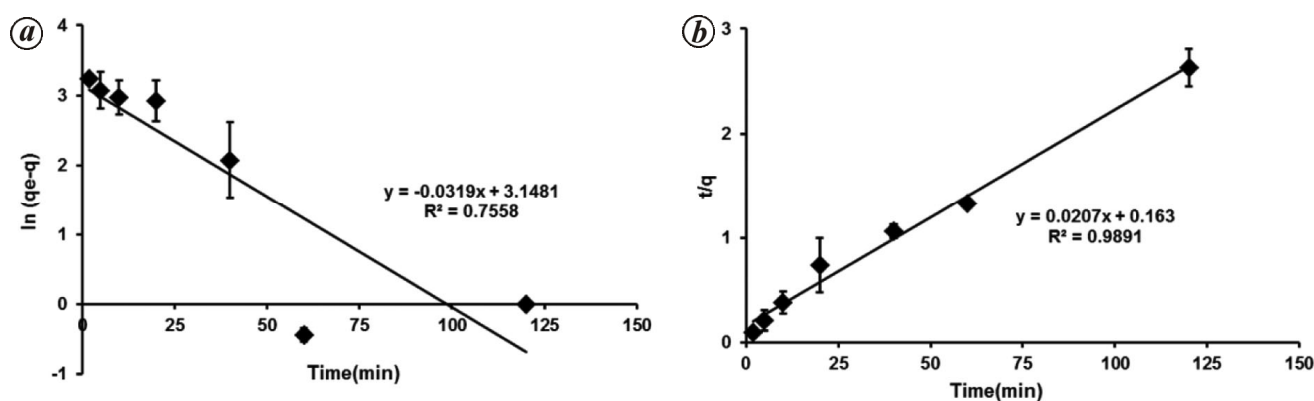
Table 2 summarizes the values of rate constant for the IIMs. According to the table, the pseudo second-order model ($R^2 = 0.989$) provides a better correlation of the sorption data compared to the pseudo first-order model ($R^2 = 0.755$). The q_e value (48.309 µg/g) calculated for the second-order model is close to the q_e experimental value (45.632 µg/g), while the q_e value calculated for the first-order model is 23.292 µg/g. It can be concluded that in the tested adsorption system of IIMs for the sorption of Hg(II) ions, the pseudo second-order is the most followed

Table 1. Langmuir and Freundlich constants

q_{\max} (exp) ($\mu\text{g/g}$)	Langmuir constants			Freundlich constants		
	K_L (calc) ($\mu\text{g/g}$)	b_L (l/mg)	R^2	K_F (calc) ($\mu\text{g/g}$)	b_F (l/mg)	R^2
35.151	37.313	0.047	0.951	5.243	0.385	0.876

Table 2. Comparison of pseudo first and second order sorption rate constants

q (exp) ($\mu\text{g/g}$)	Sorption rate constants					
	First order			Second order		
	k_1 (min^{-1})	q_e (calc) ($\mu\text{g/g}$)	R^2	k_2 ($\text{g } \mu\text{g}^{-1} \text{min}^{-1}$)	q_e (calc) ($\mu\text{g/g}$)	R^2
45.632	0.032	23.292	0.755	0.127	48.309	0.989

**Figure 11.** (a) Pseudo first-order and (b) pseudo second-order kinetic models for the sorption of Hg(II) ions by the IIMs.

pathway compared to the pseudo first-order. Further, the rate-limiting step may be the chemical sorption step that involves the transfer/exchange of valence electrons between the adsorbate and the adsorbent²¹.

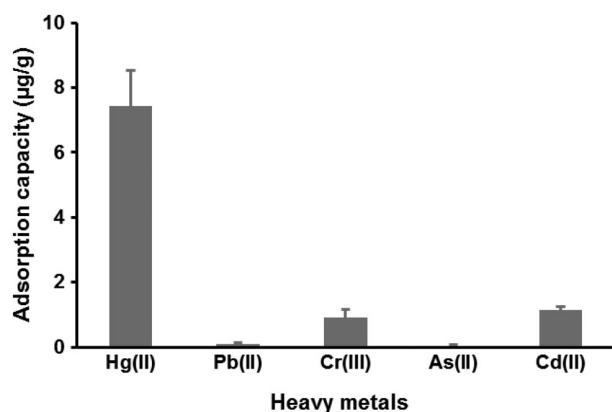
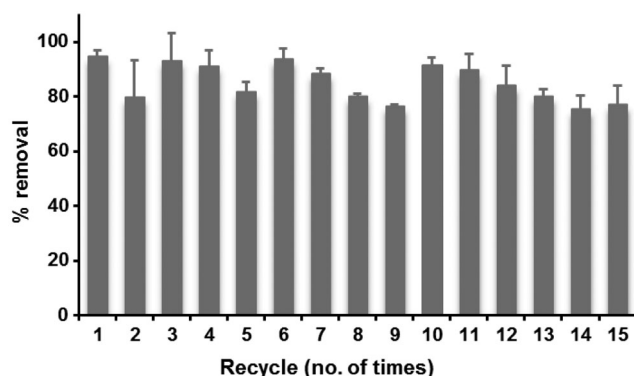
Selectivity study: Selectivity and specificity are the key factors in determining the effectiveness of an imprinted polymer. In order to prove the selectivity of IIMs, competitive adsorption of Pb(II), Cd(II), As(II) and Cr(III) towards Hg(II) ions from their model mixture was also investigated. The selected metal ions present in 0.1 l of the total volume of mixture solution (consisting of 10 $\mu\text{g/l}$ of concentration of every metal ion) were equilibrated with 0.1 g of IIMs. The adsorption capacity of Hg(II), Pb(II), Cd(II), As(II) and Cr(III) was found to be 7.43, 0.11, 1.15, 0.00 and 0.92 $\mu\text{g/g}$ respectively (Figure 12). These values show that the Hg(II) ions have highest adsorption capacity compared to other metal ions. This indicates that the IIMs have good selectivity towards the target ions (Hg(II)) even in the presence of other competitive metal ions. This may be due to the presence of memory cavities with specific size, structure, shape and binding interaction of IIM sites to the target ions²².

Recycle test: The reusability or recycle test of the IIMs for removal of Hg(II) ions was investigated. After each removal test, the IIMs were washed with 0.05% of thio-urea for recycling. Figure 13 shows the percentage removal of Hg(II) by the IIMs for 15 cycles. The graph shows the percentage removal of Hg(II) ions by the IIMs in the range 94.33% to 76.76% for 15 cycles. Clearly, the IIM tablets exhibited high adsorption ability towards Hg(II) ions even after 15 cycles, thereby confirming no losses in 'memory effect' (memory of active sites of Hg(II) ions)²³. Thus, it indicates that the IIMs are stable and can serve as good adsorbents.

Testing of real-time aqueous samples: The developed material was tested for its efficacy in terms of removal of the Hg(II) ions from river water, industrial waste water and condensate samples. The recovery of Hg(II) ions from river, industrial waste and condensate waters was found to be 82.1%, 31.03% and 9.9% respectively (Table 3). This indicates that the IIMs reveal much higher recovery and recognition ability towards Hg(II) ions in river water (aqueous phase) than in the industrial waste and condensate waters. This may be due to the fact that

Table 3. Percentage removal of Hg(II) ions by the IIMs obtained from real-time industrial samples

Sample	Before treatment ($\mu\text{g/l}$)	After treatment ($\mu\text{g/l}$)	Removal (%)
River water (mining of bauxite industry)	249.101	44.587	82.10 ± 11.00
Waste water (petroleum industry)	13.308	9.179	31.03 ± 6.18
Condensate (petroleum industry)	3.455	3.113	9.90 ± 2.28

**Figure 12.** Selectivity study of Hg(II) ions by the IIMs in the presence of foreign ions (experimental conditions: 0.1 g of IIMs; C_i of each metal ion $10 \mu\text{g/l}$; volume 0.1 l; pH 4.7; room temperature).**Figure 13.** Removal of Hg(II) percentage for recycle test of the IIMs (experimental conditions: 0.1 g of IIMs; $C_{\text{Hg(II)}}$ $10 \mu\text{g/l}$; volume 0.1 l; pH 4.7; room temperature).

the river water has similar properties and viscosity with the standard aqueous solution of Hg(II) ions. In addition, the industrial waste and condensate water samples contain many other species such as organic compounds, salts and other metals which have the ability to disturb the interference of Hg(II) ions with the ion imprinting sites during rebinding process²⁴.

Conclusion

IIMs in tablet form for the selective removal of Hg(II) ions in aqueous industrial samples were successfully prepared using the moulding technique. The prepared poly-

mer material was characterized for its physical properties by means of FTIR, TGA, FESEM and BET analysis. From the pH-dependent studies, maximum adsorption was found to take place at pH of 4.7. In addition, studies of adsorption isotherms showed that the Langmuir isotherm was preferably followed compared to the corresponding Freundlich isotherm. Also, the adsorption kinetic study indicated that the pseudo second-order pathway seems to fit well against the pseudo first-order pathway during the Hg(II) ions adsorption process. Further, the most important characteristic feature of the IIMs was their excellent selectivity towards the Hg(II) ions, when other competitive metal ions like Cd(II), Cr(III), Pb(II) and As(II) were present. In addition, we found that the IIM adsorbent had good reusability and could be used more than 15 times for adsorbing Hg(II) ions from aqueous samples. Finally, the efficiency of IIMs towards river, industrial waste and condensate water samples showed that the prepared IIMs in tablet form had specific recognition capability, high recovery and excellent reusability for the removal of Hg(II) ions.

Conflict of interest. The authors declare no conflict of interest with this work.

- Miretzky, P. and Cirelli, A. F., Hg(II) removal from water by chitosan and chitosan derivatives: a review. *J. Hazard. Mater.*, 2009, **167**, 10–23.
- Gaulier, F. *et al.*, Mercury speciation in liquid petroleum products: comparison between on-site approach and lab measurement using size exclusion chromatography with high resolution inductively coupled plasma mass spectrometric detection (SEC-ICP-HRMS). *Fuel Process. Technol.*, 2015, **131**, 254–261.
- Rodríguez, O., Padilla, I., Tayibi, H. and López-Delga, A., Concerns on liquid mercury and mercury-containing wastes: a review of the treatment technologies for the safe storage. *J. Environ. Manage.*, 2012, **101**, 197–205.
- Wang, J., Feng, X., Anderson, C. W., Xing, Y. and Shang, L., Remediation of mercury contaminated sites – a review. *J. Hazard. Mater.*, 2012, **221–222**, 1–18.
- Wilhelm, S. M. and Bloom, N., Mercury in petroleum. *Fuel Process. Technol.*, 2000, **63**, 1–27.
- Wilcox, J. *et al.*, Mercury adsorption and oxidation in coal combustion and gasification processes. *Int. J. Coal Geol.*, 2012, **90–91**, 4–20.
- Ganjali, M. R., Alizadeh, T., Azimi, F., Larjani, B., Faridbod, F. and Norouzi, P., Bio-mimetic ion imprinted polymer based potentiometric mercury sensor composed of nano-materials. *Int. J. Electrochem. Sci.*, 2011, **6**, 5200–5208.
- Liu, Y., Chang, X., Yang, D., Guo, Y. and Meng, S., Highly selective determination of inorganic mercury(II) after preconcentration

- with Hg(II)-imprinted diazoaminobenzene-vinylpyridine copolymers. *Anal. Chim. Acta*, 2005, **538**, 85–91.
9. Singh, D. K. and Mishra, S., Synthesis and characterization of Hg(II)-ion-imprinted polymer: kinetic and isotherm studies. *Desalination*, 2010, **257**, 177–183.
 10. Xingliang, S., Jinhua, L., Jiangtao, W. and Lingxin, C., Quercetin molecularly imprinted polymers: preparation, recognition characteristics and properties as sorbent for solid-phase extraction. *Talanta*, 2009, **80**, 694–702.
 11. Haginaka, J. and Sanbe, H. J., Uniformly sized molecularly imprinted polymer for (*S*)-naproxen: retention and molecular recognition properties in aqueous mobile phase. *J. Chromatogr. A*, 2001, **913**, 141–146.
 12. Chen, Z. Y., Zhao, R., Shangguan, D. H. and Liu, G. Q., Preparation and evaluation of uniform-sized molecularly imprinted polymer beads used for the separation of sulfamethazine. *Biomed. Chromatogr.*, 2005, **19**, 533–538.
 13. Ye, L., Weiss, R. and Mosbach, K., Synthesis and characterization of molecularly imprinted microspheres. *Macromolecules*, 2000, **33**, 8239–8245.
 14. Glad, M., Reinholdsson, P. and Mosbach, K., Molecularly imprinted composite polymers based on trimethylolpropanetriacrylate (TRIM) particles for efficient enantiomeric separations. *React. Polym.*, 1995, **25**, 47–54.
 15. Liu, X., Ouyang, C., Zhao, R., Shangguan, D., Chen, Y. and Liu, G., Monolithic molecularly imprinted polymer for sulfamethoxazole and molecular recognition properties in aqueous mobile phase. *Anal. Chim. Acta*, 2006, **571**, 235–241.
 16. Tumin, N. D., Chuah, A. L., Zawani, Z. and Rashid, S. A., Adsorption of copper from aqueous solution by ElaisGuineensis kernel activated carbon. *J. Eng. Sci. Technol.*, 2008, **3**(2), 180–189.
 17. dos Santos, V. C. G., Grassi, M. T. and Abate, G., Sorption of Hg (II) by modified K10 montmorillonite: influence of pH, ionic strength and the treatment with different cations. *Geoderma*, 2015, **237**, 129–136.
 18. Thakur, S., Kumari, S., Dogra, P. and Chauhan, G. S., A new guar gum-based adsorbent for the removal of Hg(II) from its aqueous solutions. *Carbohydr. Polym.*, 2014, **106**, 276–282.
 19. Rahchamani, J., Mousavi, H. Z. and Behzad, M., Adsorption of methyl violet from aqueous solution by polyacrylamide as an adsorbent: isotherm and kinetic studies. *Desalination*, 2011, **267**(2), 256–260.
 20. Kavitha, D. and Namasivayam, C., Experimental and kinetic studies on methylene blue adsorption by coir pith carbon. *Bioresour. Technol.*, 2007, **98**, 14–21.
 21. Ong, S. T., Lee, C. K. and Zainal, Z., Removal of basic and reactive dyes using ethylenediamine modified rice hull. *Bioresour. Technol.*, 2007, **98**, 2792–2794.
 22. Komiyama, M., Takeuchi, T., Mukawa, T. and Asanuma, H., *Molecular Imprinting from Fundamentals to Applications*, Wiley-VCH Verlag GmbH & Co. KGaA, Weinheim, Germany, 2003.
 23. Svenson, J. and Nicholls, I. A., On the thermal and chemical stability of molecularly imprinted polymers. *Anal. Chim. Acta*, 2001, **435**, 19–24.
 24. UK Essays. November 2013; <https://www.ukessays.com/essays/environmental-sciences/mercury-problems-in-oil-and-gas-industries-environmental-sciences-essay.php?cref=1> (accessed on 30 April 2017).

ACKNOWLEDGEMENTS. We thank the Ministry of Higher Education, Malaysia for financial support in the form of Prototype Research Grant Scheme (PRGS) and My Brain 15. F.M. acknowledges the Deanship of Scientific Research, King Saud University, Saudi Arabia for funding through Vice Deanship of Scientific Research Chairs.

Received 26 January 2017; revised accepted 23 June 2017

doi: 10.18520/cs/v113/i12/2282-2291